HHS Public Access

Author manuscript

Cancer Immunol Res. Author manuscript; available in PMC 2020 October 27.

Published in final edited form as:

Cancer Immunol Res. 2018 October ; 6(10): 1274–1287. doi:10.1158/2326-6066.CIR-18-0065.

CD30-Redirected Chimeric Antigen Receptor T Cells Target CD30+ and CD30− Embryonal Carcinoma via Antigen-dependent and Fas/FasL Interactions

Lee K. Hong[1], **Yuhui Chen**[2], **Christof C. Smith**[1], **Stephanie A. Montgomery**[3], **Benjamin G. Vincent**[4], **Gianpietro Dotti**[1,4], **Barbara Savoldo**[2,4]

[1]Department of Microbiology and Immunology, University of North Carolina at Chapel Hill

[2]Department of Pediatrics, University of North Carolina at Chapel Hill

[3]Department of Pathology and Laboratory Medicine, University of North Carolina at Chapel Hill

[4]Lineberger Comprehensive Cancer Center, University of North Carolina at Chapel Hill

Abstract

Tumor antigen heterogeneity limits success of chimeric antigen receptor (CAR) T-cell therapies. Embryonal carcinomas (ECs) and mixed testicular germ cell tumors (TGCTs) containing EC, which are the most aggressive TGCT subtypes, are useful for dissecting this issue as ECs express the CD30 antigen but also contain $CD30^{-/dim}$ cells. We found that CD30-redirected CAR T cells (CD30.CAR T cells) exhibit antitumor activity *in vitro* against the human EC cell lines Tera-1, Tera-2 and NCCIT, and putative EC stem cells identified by Hoechst dye staining. Cytolytic activity of CD30.CAR T cells was complemented by their sustained proliferation and pro-inflammatory cytokine production. CD30.CAR T cells also demonstrated antitumor activity in an *in vivo* xenograft NSG mouse model of metastatic EC. We observed that CD30.CAR T cells, while targeting $CD30^+$ EC tumor cells through the CAR (i.e. antigen-dependent targeting), also eliminated surrounding $CD30^-$ EC cells in an antigen-independent manner, via cell-cell contact-dependent Fas/FasL interaction. In addition, ectopic Fas (CD95) expression in $CD30^+$ Fas^- EC was sufficient to improve CD30.CAR T-cell antitumor activity. Overall, these data suggest that CD30.CAR T cells might be useful as an immunotherapy for ECs. Additionally, Fas/FasL interaction between tumor cells and CAR T cells can be exploited to reduce tumor escape due to heterogeneous antigen expression or to improve CAR T-cell antitumor activity.

Introduction

Immunotherapy is useful in the battle against cancer. Immunotherapies range from monoclonal antibody (mAb)-based therapies, for example in the form of immunotoxin conjugates or checkpoint inhibitors, to the adoptive transfer of *ex vivo* expanded tumor-specific T cells, whose antigen specificity is mediated by their native TCR, by transgenic

Corresponding Author: Barbara Savoldo, Address: 125 Mason Farm Road, Marsico Hall 5203, Chapel Hill, NC 27599-7290, Phone: 919-962-8414, bsavoldo@med.unc.edu.

Conflict of Interest Statement: The authors have declared that no conflict of interest exists.

TCR, or by chimeric antigen receptors (CARs). CARs are chimeric proteins in which an Ab single-chain variable fragment (scFv), as an extracellular receptor, is fused with T-cell effector and co-stimulatory intracellular domains (1). CAR-based technology overcomes some of the limitations of mAb-based immunotherapy because CARs combine the antigen specificity of a mAb with intrinsic properties of T lymphocytes (2). In contrast to mAbs, CAR-expressing T lymphocytes (CAR T cells) can persist long-term, migrate to the tumor site following gradients of chemokines such as CXCL12 (3), and exploit multiple lytic functions (4).

One cause of tumor escape and relapse after targeted immunotherapy, including immunotherapy by CAR T cells, is the heterogeneous expression of target antigens within the tumor. For example, some patients with leukemia showed emergence of $CD19^{-}$ leukemic cells after adoptive transfer of CD19-specific CAR T cells due to selection pressure of alternatively spliced CD19 isoforms (5). Similarly, tumor escape due to antigen loss has been observed in patients with glioblastoma treated with EGFRvIII-specific CAR T cells (6). Bispecific CAR T cells that target two antigens simultaneously (7) can reduce tumor escape, but may also increase the risk of toxicities in normal tissues due to on-target off-tumor effects, especially in solid tumors, which frequently share antigens with normal tissues. There is a need to overcome tumor escape associated with antigen heterogeneity, especially as these otherwise successful immunotherapies move from liquid cancers into the arena of solid tumors.

Testicular germ cell tumors (TGCTs), sub-categorized as seminomas and non-seminomas (NS-TGCTs), are the most common malignancies in male adolescents and young adults (8). Pure embryonal carcinomas (EC), a subtype of NS-TGCTs derived from malignant embryonic stem cells, accounts for 2% of all TGCTs (9). More commonly, EC is a histologic component in 85% of mixed TGCTs in which multiple subtypes are present (9). The presence of EC is associated with poor outcomes (3). CD30, a TNF superfamily member with a pro-survival role in transformed stem cells (10), characterizes ECs at diagnosis and at relapse (11). Furthermore, the persistence of $CD30^{+}$ tumor cells post-chemotherapy is considered a negative prognostic factor (11). Therefore, CD30-targeting immunotherapy may improve overall survival while reducing chemotherapy-associated morbidities. We have therefore used CD30-redirected CAR T cells (CD30.CAR T cells), a validated approach in patients with Hodgkin's lymphomas and $CD30^{+}$ non-Hodgkin's lymphomas (12;13), to test both the efficacy and challenges of CAR T cells as an immunotherapy for TGCTs.

Materials and Methods

Tumor cell lines.

The Hodgkin's lymphoma-derived cell line HDLM-2 was obtained from the German Collection of Cell Cultures (DMSZ, Braunschweig, Germany). The Burkitt's lymphoma-derived cell line Raji, the EC-derived cell lines NCCIT, Tera-1, and Tera-2, the neuroblastoma-derived cell lines Lan-1 and SH-SY5Y, and the leukemia-derived cell line K562 were obtained from American Type Culture Collection (ATCC). K562 cells and Lan-1 cells were transduced with a retroviral vector encoding either human CD19 or CD30 to

constitutively express CD19 or CD30, respectively. For CD95 overexpression in NCCIT cells, the full-length human CD95 was cloned into the retroviral vector pLXSN. CD95 siRNA pSUPER vectors were used for CD95 knockdown in Tera-1 cells as described (14). Tumor cells or CD30.CAR T cells were labeled with the retroviral vector encoding eGFP-Firefly-Luciferase (eGFP-FFLuc) for *in vivo* studies (15). Raji, K562, Lan-1, SH-SY5Y and NCCIT cells were maintained in culture with RPMI 1640 medium (Gibco) supplemented with 10% fetal bovine serum (Corning), 1X penicillin-streptavidin (Invitrogen), and 2 mM GlutaMax (Invitrogen). Tera-1 and Tera-2 cells were maintained with McCoy's 5A media (Corning) with 15% FBS, 1X penicillin-streptavidin, and 2 mM GlutaMax. Cells were maintained in culture in a humidified atmosphere containing 5% CO_2 at 37°C. Cells were kept in culture for less than 6 consecutive months, after which aliquots from the original expanded vial were used. Tumor cell lines were routinely tested to exclude contamination with mycoplasma and assessed for the expression of CD30 or GD2 by flow cytometry to confirm identity.

Retroviral constructs and transduction of T lymphocytes.

We constructed two second-generation CD30.CARs on an SFG retroviral vector backbone encoding either the CD28 (CD30.28) or 4–1BB (CD30.BB) endodomains coupled with the CD3ζ endodomain (Supplementary Fig. S1A) using the previously reported CD30-specific scFv (16). Non-transduced T cells from matched independent experiments or T cells transduced with a CD19.CAR encoding the CD28 endodomain (17) were used as controls (control T cells) for *in vitro* and *in vivo* experiments, respectively. Transient retroviral supernatants were produced using 293T cells as previously described (16). Peripheral blood mononuclear cells isolated from independent experiments with buffy coats of healthy volunteer blood (Gulf Coast Regional Blood Center, Houston, TX) were transduced to express the CD30.CARs, GD2.CAR, or CD19.CAR and maintained in culture as previously described (18).

Flow cytometry.

The following mAbs conjugated with phycoerythrin (PE), peridinin-chlorophyll-protein complex (PerCP), fluorescein isothiocyanate (FITC), allophycocyanin (APC), APC-H7, Alexa Fluor 647 (AF 647), Alexa Fluor 700, Brilliant Violet (BV) 421, BV 711, and/or peridinin chlorophyll protein (Per-CP) were used: CD3, CD4, CD8, CD30 (Clone Ber-H3), CD33, CD45, CD45RA, CD45RO, CD95, CD276 (B7H3), CCR7, GD2 (Clone 14.G2a) and active caspase 3 (BD Biosciences). Rabbit antibody to cleaved caspase 7 and Alexa Fluor 488-conjugated goat anti-rabbit IgG mAbs were purchased from Cell Signaling Technologies. Annexin V/7AAD staining was performed according to manufacturer's instructions (BD Biosciences). CAR expression by T cells was detected using an Alexa Fluor 647 conjugated goat anti-mouse F(ab')2 antibody (Jackson Immuno). For T-cell immunophenotypes, samples were labeled in a two-step process by anti-F(ab')2 antibody followed by washing in PBS and adding T-cell marker antibodies. To detect CD19.CAR we used a specific anti-idiotype antibody (Clone 233–4A) generated by immunizing mice with the anti-CD19 scFv followed by APC-conjugated rat anti-mouse IgG secondary mAb (BD Biosciences). To detect GD2.CAR we used a specific anti-idiotype antibody 1A7 (19). For absolute number calculations, samples were analyzed using CountBright absolute counting

beads (Thermo Fisher). For intracellular staining, cells were stained with surface antibodies, washed and fixed with Cytofix/Cytoperm (BD), followed by intracellular staining in 1X permeabilization buffer per manufacturer's instructions. Samples were acquired with at least 10,000 positive events using a FACSCanto II flow cytometer (BD) and analyzed by FlowJo (Treestar). FACS sorting was also performed using CD30-PE or CD95-PE labeled tumor cells on an Aria III flow cytometer (BD; UNC Flow Cytometry Core Facility).

Side Population (SP) staining by Hoechst dye/Dye Cycle Violet and cell sorting.

For SP analysis, cells were incubated in HBSS (Life Technologies) containing 2% FBS, 10 mM HEPES (Life Technologies), and either 10 μg/mL Hoechst 33342 (Sigma-Aldrich) or 10 μM Vybrant DyeCycle Violet (DCV) (Life Technologies) for 90 min at 37°C. Cells were then washed with ice cold HBSS and FACS sorted or labeled with CD30-PE for flow cytometry analysis. To detect the SP fluorescent phenotype, Hoechst 33342 samples were excited using a 355nm UV laser on a LSRII/Fortessa flow cytometer (BD) while DCV samples were excited using a 405 nm violet laser on an Aria III flow cytometer. Corresponding band-pass filter sets were: blue 450–50 bp/450 LP, 610–20 bp/690 LP (LSRII/Fortessa) and 450–50 bp/502 LP (Aria III).

Cytotoxicity assay.

The cytotoxic activity of transduced effector cells was evaluated using a 6-hour ^{51}Cr release assay as previously described (16). Labeled target cells were: Raji ($CD30^{-}$), HDLM-2 ($CD30^{+}$), Tera-2, and NCCIT.

In vitro coculture.

Adherent tumor cell lines were plated at 0.1 – 0.25 × 10^6 cells/mL in a 24-well tissue culture plate one day prior to the addition of CD30.CAR T cells or CD19.CAR T cells at various effector/target (E:T) ratios. After five days, cells were collected using Versene (UNC Tissue Culture Facility) for non-enzymatic dissociation of tumor cells, washed in PBS, labeled with fluorescent CD3-APCH7 and CD30-FITC mAbs and analyzed by flow cytometry. In experiments with Lan-1/WT or Lan-1/CD30 control tumor cells, remaining cells were labeled with CD3-APCH7 and GD2-PE mAbs. For GD2.CAR and SH-SY5Y coculture experiments, remaining cells were labeled with CD3-PerCP, CD276-BV421, and GD2-PE mAbs. In experiments where CD19.CAR T cells and K562 cells were used, remaining cells were also labeled with CD33-APC mAb. Transwell assays were performed using 0.4 μm transwells (EMD Millipore) in 24-well tissue culture plates. Tera-1 cells were also cultured with coculture supernatant collected at 24hrs or human recombinant IFNγ or TNFα (Peprotech) and analyzed for CD30 expression by flow cytometry after 48hrs in culture. For detecting T-cell apoptosis *in vitro*, control T cells or CD30.CAR T cells were cocultured with Tera-1/WT or Tera-1/CD95 KD cells at a 1:1 ratio or with anti-Fas agonistic Ab (clone CH11, Sigma Aldrich) in low-serum media (2% FBS) (14) for 72hrs followed by Annexin V/7AAD staining.

Carboxyfluorescein succinimidyl ester (CFSE)-based proliferation assay.

CD30.CAR T cells and control T cells were labeled with CFSE (Invitrogen) and cocultured with tumor cells at 5:1 E:T ratio. On day 5, cells were collected, labeled with CD3-APCH7, CD4-PECy7, and CD8-APC mAbs (BD Biosciences), and analyzed for CFSE dilution by flow cytometry. In separate coculture experiments, tumor cells were labeled with CFSE and plated one day prior to the addition of control T cells and CD30.CAR T cells. Five days later cells were collected and $CFSE^+$ tumor cells were identified by flow cytometry.

Enzyme-linked immunosorbent assay (ELISA).

The release of IL-2 and IFNγ by CD30.CAR T cells was quantified using specific ELISAs (R&D Systems) in supernatants collected after 24 hours from T cells cocultured with tumor cells.

Reverse transcription quantitative polymerase chain reaction.

Cells were lysed and RNA was extracted using the RNeasy Mini kit (Qiagen) and reverse transcribed into cDNA (Superscript VILO, Invitrogen). Human ABCG2 (Hs01053790_m1), SOX2 (Hs01053049_s1), and CD95L (Hs00181226_g1) mRNA expression was quantified using Taqman probes (Catalog # 4331182, ThermoFisher Scientific) on a Quantstudio 6 PCR machine (Applied Biosystems) using β-actin as housekeeping gene control (Invitrogen).

Xenograft mouse models.

All mouse experiments were performed in accordance with UNC Animal Husbandry and Institutional Animal Care and Use Committee (IACUC) guidelines and were approved by UNC IACUC. To measure *in vivo* the growth of EC cells, we used two orthotopic models in NOD/SCID/γcnull (NSG) male mice ages 6 to 12 weeks. In the first model, Tera-2 eGFP-FFLuc cells were resuspended in DPBS (Corning) and injected directly into the left testis (2×10^6 cells/mice) (20). In the second model, Tera-2 eGFP-FFLuc cells were resuspended in Matrigel (Corning) and engrafted under the left kidney capsule (0.25×10^6 cells/mice) (21). To assess antitumor activity of CD30.CAR T cells, mice received T cells (1×10^7 cells/mouse) intravenously via tail vein injection 14 days later, when the bioluminescence emission (BLI) of the tumor was consistently measurable. To monitor T-cell localization and expansion, mice were engrafted with wild-type (WT) Tera-2 cells and infused 21 days later with 1×10^7 control or CD30.CAR T cells transduced with eGFP-FFLuc. The IVIS imaging system (Xenogen; UNC Biomedical Imaging Research Center) was used to monitor tumor growth or T-cell expansion and localization. Briefly, a constant region of interest was drawn over the tumor regions and the intensity of the signal measured as total flux (photon/sec) as previously described (21).

Mouse tissue processing and immunohistochemistry (IHC).

T cell-treated mice with tumor engrafted in kidney or testis were sacrificed and tumors were fixed in 10% neutral buffered formalin (Fisher Scientific), processed in 3 μm longitudinal planes, and stained for hematoxylin/eosin (H&E) and a human CD3 antibody (UNC Lineberger Animal Histopathology Core Facility). Blood samples normalized to 100μL total

volume and spleen samples were also harvested, lysed to remove red blood cells (ACK Lysis Buffer, Gibco), and stained with anti-human CD45 and CD3 for detection of T cells. For detection of CD30, mouse tissues and human testes tissue arrays (US Biomax) were stained with a human CD30 antibody(Clone Ber-H2, Dako; UNC Translational Pathology Laboratory). H score is the cumulative score of the frequency of positive cells x score calculated by a membrane staining algorithm, which scores cells based on membrane staining intensity (UNC Translational Pathology Laboratory). Tumors collected from tumor bearing mice were counted by a board-certified veterinary pathologist (S. Montgomery) blinded to experimental conditions. A random tumor field containing at least 80% tumor and positively labeled CD3 cells was selected and, depending on tumor size, up to ten high power (400X) fields of view were examined using a grid matrix approach (21). Two samples from mice treated with either CD30.28 T cells or CD30.BB T cells had sheets of positive cells that were too numerous to count (TNTC) and were not included in the quantitative analysis.

RNA-Seq.

Briefly, total RNA was extracted from EC cell lines and mRNA libraries were prepared (TruSeq Stranded mRNA Library Prep, Illumina) and sequenced on the Illumina HiSeq4000 platform (UNC High-Throughput Sequencing Facility) using paired-end 100-bp reads, with 84 million reads on average (range 49–139 million). RNA-seq data was aligned with STAR alignment (v2.4.2) and quantified with Salmon (v0.6.0). Differential gene expression analysis was performed using the R DESEq2 package (https://genomebiology.biomedcentral.com/articles/10.1186/s13059-014-0550-8). Among all significantly expressed genes between NCCIT, TERA1, and TERA2 cell lines (FDR p-value < =0.05), expression was further filtered to genes contained within the KEGG Apoptosis and the Biocarta p53 pathway signatures (https://www.ncbi.nlm.nih.gov/pubmed/10592173; https://doi.org/10.1089/152791601750294344).

Statistical analysis.

All *in vitro* data are presented as mean ± SEM. A two-sided, paired Student's T test was used to determine the statistical significance of differences between groups, and p-values less than .05 were accepted as indicating a significant difference. When multiple comparison analyses were required, statistical significance was evaluated by one-way ANOVA or repeated-measures ANOVA for matched T-cell independent experiments followed by two-sided paired Student's *t* test as needed for comparing two groups. Statistical significance for differences in tumor growth *in vivo* were evaluated by one-way ANOVA. Differences in survival curves for mouse experiments were compared by log-rank (Mantel-Cox) test.

Results

EC cell lines and TGCT tissue specimens express CD30.

We assessed the expression of CD30 in three human EC cell lines (Tera-1, Tera-2, and NCCIT) by flow cytometry, and used wild type Lan-1 (Lan-1/WT) and $CD30^+$ Lan-1 (Lan-1/CD30) cells as negative and positive controls, respectively. The HDLM-2 Hodgkin's lymphoma cell line that constitutively expresses CD30 (22) was also used as a positive

control. All EC cell lines expressed CD30 but also contained a fraction of $CD30^{-/dim}$ cells, which were more prominent in the Tera-1 cell line (Fig. 1A). We next examined CD30 expression by immunohistochemistry (IHC) in human tissue microarrays (TMA) that include normal testes, seminomas, and NS-TGCTs. Normal testes and seminomas did not display CD30 staining (Fig. 1B). In contrast, up to 70% of EC specimens exhibited a moderate to strong, granular, membranous and Golgi CD30 staining pattern (Fig. 1B). When the pattern of CD30 expression was scored using computational analysis and analyzed as H score (Fig. 1C) or as frequency of positive cells (Fig. 1D), CD30 was routinely expressed only by primary ECs ($p<0.001$, one-way ANOVA), although with some heterogeneity.

CD30.CAR T cells target $CD30^+$ EC cell lines and their side population (SP) cells.

We engineered T cells to express either CD30.28 or CD30.BB CARs (Supplementary Fig. S1A). Transduction efficiency was consistently >90% for both constructs (Supplementary Fig. S1B), and CD30.CAR T cells expanded *in vitro* in the presence of cytokines (Supplementary Fig. S1C). CD30.CAR T cells showed phenotypic characteristics of stem cell-like, effector-memory and central-memory T cells (Supplementary Fig. S1D).

CD30.CAR T cells lysed $CD30^+$ HDLM-2 and Tera-2 tumor cells at higher frequencies compared to control T cells (Ctr.Ts), whereas $CD30^-$ Raji tumor cells were spared in short-term ^{51}Cr release assays (Fig. 2A). CD30.CAR T cells also eliminated $CD30^+$ tumor cells in long-term coculture experiments. CD30.CAR T cells targeted Lan-1/CD30 cells whereas neither control T cells nor CD30.CAR T cells eliminated Lan-1/WT cells (Supplementary Fig. S2A). Using effector:target (E:T) ratios ranging from 1:5 to 5:1, both CD30.28 T cells and CD30.BB T cells exhibited antitumor activity against all three EC cell lines tested (Fig. 2B–D and Supplementary Fig. S2B–D). Although CD30.CAR T cells eliminated Tera-1 (Fig. 2B and Supplementary Fig. S2B) and Tera-2 (Fig. 2C and Supplementary Fig. S2C) cells at low E:T ratios (1:1, 1:2 and 1:5), they could only control NCCIT-cell growth at the highest 5:1 E:T ratio (Fig. 2D). EC tumor cells do not express the co-stimulatory molecules CD80 and CD86, and thus do not provide costimulation to T cells (Supplementary Fig. S2E–F). Both CD30.28 T cells and CD30.BB T cells showed proliferation in response to EC cells, as assessed by CFSE dilution assays (Supplementary Fig. S3A), confirming both endodomains provided co-stimulation. Additionally, CD30.CAR T cells secreted IFNγ and IL-2 upon stimulation with EC cells (Supplementary Fig. S3B,C). In summary, CD30.CAR T cells showed selective activation by $CD30^+$ EC cells and antitumor activity *in vitro*.

Cancer stem cells are a subpopulation of tumor cells with stem cell characteristics that can contribute to tumor relapse (23). Taking in consideration the germinal origin of ECs, we asked whether EC cell lines contain putative cancer stem cells using the Hoechst 33342 staining for detection of SP cells (24). Although all EC lines had some SP cells, Tera-1 cells showed the highest frequency of SP cells (15–30%) (Fig. 3A). SP cells retained expression of CD30 (Fig. 3A) and exhibited cancer stem cell characteristics based on the expression of the stem cell-associated markers ABCG2 (25) and SOX2 (26) (Fig. 3B), and their capacity to differentiate to non-SP cells (24) (Fig. 3C). CD30.CAR T cells targeted sorted SP cells in coculture assays (Fig. 3D). Therefore, CD30.CAR T cells can target both differentiated and stem cell-like $CD30^+$ EC cells.

CD30.CAR T cells localize to EC tumors and exhibit antitumor activity *in vivo.*

To model EC *in vivo*, we inoculated NSG mice with luciferase-labeled Tera-2 tumor cells directly into the testes (20). Tera-2 cells engrafted, as detected by bioluminescence (BLI) (Fig. 4A) and retained expression of CD30 *in situ* as assessed by IHC (Fig. 4B). However, tumors engrafted in mouse testes rarely metastasized to extragonadal sites. As intraperitoneal or intravenous administration of EC cells in NSG mice resulted in poor tumor engraftment and because metastatic TGCTs typically arise in midline locations and retroperitoneum (27), we engrafted Tera-2 cells orthotopically under the kidney capsule as a clinically relevant model of metastatic EC. In this tumor model, luciferase-labeled CD30.CAR T cells injected intravenously via tail vein (i.v.) localized and accumulated at the tumor site. Although CD30.BB T cells showed increased accumulation early after injection, CD30.28 T cells showed better long-term persistence compared to that of controls (control T cells) or CD30.BB T cells (Fig. 4C and Supplementary Fig. S4A). T cells were detectable in the blood (Supplementary Fig. S4B) and spleen (Supplementary Fig. S4C) in all treatment groups between day 30–45 post T-cell infusion. When analyzed by IHC, tumors were located under the renal capsule, sometimes infiltrating into the subjacent cortex or deeper into the medulla (Supplementary Fig. S4D). In tumor specimens collected between day 30–45 post T-cell infusion, we observed infiltrating $CD3^+$ T cells that occasionally formed small clusters (Supplementary Fig. S4D). No significant differences in $CD3^+$ T-cell infiltration between control T cells and CD30.CAR T-cell treated groups were observed (Fig. 4D), likely because the analysis was performed between day 49–56 post tumor inoculation when tumor burden is significantly different between groups.

To test CD30.CAR T-cell activity, luciferase-labeled EC cells were engrafted in the kidney and tumor growth measured by BLI. When tumors in the kidney showed consistent increase in BLI, mice received i.v. unlabeled control T cells or CD30.CAR T cells. Both CD30.28 T cells and CD30.BB T cells reduced the tumor growth compared to control T cells (Fig. 4E and Supplementary Fig. S4E), but CD30.28 T cells supported better survival when using tumor BLI of 5×10^7 p/s as a survival cutoff (Fig. 4F).

$CD30^-$ EC cells eliminated by CD30.CAR T cells through cell-cell contact process.

Although not displaying lytic activity against $CD30^-$ tumor cells alone in short-term (Fig. 2A) or long-term (Supplementary Fig. S2A) assays, CD30.CAR T cells eliminated Tera-1 cells, which contain a mixture of $CD30^+$ and $CD30^-$ cells (Fig. 1A), in 5-day coculture assays (Fig. 2B). To dissect this phenomenon, we cocultured CD30.CAR T cells with $CD30^-$ flow-sorted Tera-1 cells (Fig. 5A) and found that they were no longer eliminated (Fig. 5B and Supplementary Fig. S5A), with no detectable IFNγ or IL-2 released in culture supernatants (Supplementary Fig. S5B). In addition, when unselected Tera-1 cells were cocultured with CD30.CAR T cells at low E:T ratios, $CD30^+$ Tera-1 cells were preferentially eliminated over the $CD30^-$ fraction (Fig. 5C). Similar results were observed with CD30.BB T cells (Supplementary Fig. S5C). We found no evidence of CD30 upregulation in $CD30^-$ Tera-1 cells when these cells were exposed to soluble factors released by CD30.CAR T cells such as IFNγ and TNFα, or when exposed to coculture supernatants (Supplementary Fig. S5D). By contrast, we observed that Tera-1 cells were eliminated in a CD30 antigen-independent manner by activated CAR T cells. To conclusively support this observation, we

cocultured Tera-1 cells with CD19.CAR T cells, which target the CD19 antigen that is not expressed by EC cells, in the presence of $CD19^-$ (K562/WT) or $CD19^+$ (K562/$CD19^+$) target cells to induce CAR T-cell activation. As shown in Fig. 5D, CD19.CAR T cells eliminated Tera-1 cells only in the presence of K562/$CD19^+$ cells. Furthermore, the elimination of Tera-1 cells was T cell-tumor cell contact-dependent since the antitumor effects were abolished when CD19.CAR T cells and K562/$CD19^+$ cells were separated from Tera-1 cells using a transwell (Fig. 5E). These data suggest that CD30.CAR T cells, upon activation through the CAR, can eliminate the fraction of Tera-1 cells that is $CD30^-$ in a cell-cell contact dependent, but antigen-independent mechanism.

Fas/FasL pathway mediates elimination of $CD30^-$ EC cells by CD30.CAR T cells.

Fas-FasL (CD95/CD95L) interactions between tumor cells and cytotoxic T lymphocytes contribute to tumor cell death (28). CAR T cells also upregulate FasL upon receptor engagement (29;30), and Tera-1 cells express Fas (Fig. 6A). Since the $CD30^-$ fraction of Tera-1 cells also retains Fas expression (Fig. 6B), we investigated whether CD30.CAR T cells utilize the Fas/FasL pathway to eliminate the $CD30^-$ fraction of Tera-1 cells. CD30.28 T cells upregulated FasL upon CAR engagement with EC cells after 4 hours *in vitro* (Fig. 6C). In contrast, EC cell lines did not express FasL mRNA (Supplementary Fig. S6A). When cocultured with CD30.28 T cells, the $CD30^-$ fraction of Tera-1 cells showed caspase 3 activity (Fig. 6D), which is triggered by the Fas/FasL pathway (28). By contrast, cell death of the $CD30^+$ fraction was caused by granzyme B/perforin-mediated membrane damage as detected by cleaved caspase 7 (31;32) (Fig. 6E). When CD95 was knocked down in Tera-1 cells via specific siRNA (14) (Tera-1/CD95 KD, Fig. 6F), we found reduced caspase 3 activity among $CD30^-$ Tera-1 cells compared to wildtype Tera-1 cells when cocultured with CD30.28 T cells (Fig. 6G). No difference in activation-induced cell death as measured by Annexin V/7AAD staining was observed in CD30.CAR T cells when cocultured with Fas-sufficient Tera-1 (Tera-1/WT) or Fas-knockdown Tera-1 (Tera-1/CD95 KD) cells (Supplementary Fig. S6B). Similar Fas/FasL-mediated effects were observed when the experiments were repeated using CD30.BB T cells (Supplementary Fig. S6C–F).

Ectopic Fas expression on tumor cells improves CAR T-cell activity.

To assess if the pattern of antigen-independent Fas/FasL mediated elimination of tumor cells was broadly applicable, we evaluated CD95 on the two other EC tumor cell lines Tera-2 and NCCIT. Tera-2 cells that express CD95 (Fig. 6A) were similarly targeted via antigen-independent Fas/FasL killing by CD19.CAR T cells (Supplementary Fig. S7A), but not NCCIT cells (Supplementary Fig. S7B) that lack CD95 expression (Fig. 6A). NCCIT cells appeared constitutively more resistant to CD30.CAR T cell–mediated killing (Fig. 2D and Supplementary Fig. S7C) and showed significantly decreased expression of apoptosis-related genes by RNA-Seq (including p53, Fas, and TRAIL receptor) compared to either Tera-1 or Tera-2, which showed greater coclustering of apoptosis-related gene expression patterns (Supplementary Fig. S7D and Supplementary Table S1). However, when engineered to express CD95 (NCCIT/$CD95^+$, Fig. 7A), NCCIT cells were more efficiently eliminated by CD30.28 T cells (Fig. 7B).

We further assessed whether Fas/FasL interactions are relevant for other tumor models by utilizing the neuroblastoma cell line SH-SY5Y, which contains a fraction of both $GD2^{bright}$ and $GD2^{dim}$ cells (Fig. 7C) and also lacks CD95 expression (Fig. 7D). When cocultured with GD2-redirected CAR T cells with the CD28 endodomain (GD2.28 T cells), $GD2^{bright}$ cells were eliminated, but not $GD2^{dim}$ cells (Fig. 7E). Similar to NCCIT cells, when SH-SY5Y cells were engineered to express CD95 (SH-SY5Y/$CD95^+$; Fig. 7F), these tumor cells were eliminated more readily by GD2.28 T cells (Fig. 7G). These data suggest that introducing functional Fas/FasL interactions via ectopic CD95 expression on resistant tumor cells is sufficient to improve CAR T-cell activity.

Discussion

Although CAR T-cell therapies have shown promise for treatment of hematological malignancies, barriers remain to successful use of these immunotherapies for solid tumors. Among these barriers is the diversity of expression of most targetable molecules among tumor cells, which invariably leads to tumor escape (33;34). Here, we demonstrated first the antitumor activity of CD30.CAR T cells against $CD30^+$ ECs Tera-1 and NCCIT, in support of the use of CD30.CAR T cells as a form of immunotherapy for $CD30^+$ TGCTs. Second, we discovered a mechanistic link between the lytic activity of CD30.CAR T cells (or antigen-specific CAR T cells in general) against bystander $antigen^{neg/dim}$ tumor cells and the Fas/FasL pathway. Furthermore, we showed that ectopic Fas expression in otherwise Fas^- tumor cells enhanced CAR T-cell mediated tumor elimination. Our data suggests that tumor evasion resulting from antigen loss may be compensated by the activation of the Fas/FasL pathway in CAR T cells. Our results pave the way to leverage Fas expression in ostensibly Fas^- tumor cells as a means to enhance CAR T-cell mediated tumor elimination.

Few new drugs for the treatment of ECs and TGCTs have been developed in the past few decades. Although orchiectomy is curative in patients with localized (i.e. stage 1) NS-TGCTs (35), patients with metastatic disease and those presenting with primary mediastinal tumors, even when cured, often develop long-term chemotherapy-related side effects that reduce their life expectancy (36). In addition, the outcome for patients who relapse after chemotherapy remains poor with an overall survival rate of only 30–40% (37). CD30 expression by ECs can be exploited to develop targeted therapies in these malignancies. Targeting CD30 by brentuximab vedotin, toxin-conjugated anti-CD30, has shown promising results in relapsed TGCT patients (38;39). Here we propose CD30.CAR T cells as an alternative to enhance the therapeutic index of CD30-targeted therapies in ECs, extending our previous observation in $CD30^+$ lymphomas (13). In our preclinical study using $CD30^+$ ECs, we show that CD30.CAR T cells can target human EC cell lines, localize to the tumor site *in vivo* and control tumor growth.

The presence of the EC subtype among NS-TGCTs correlates with higher rates of relapse after chemotherapy (3), which may be driven, at least in part, by the intrinsic stem cell properties of ECs (26). Cancer stem cells, which differentiate into multiple tumor cell types, are often resistant to chemotherapy and act as a reservoir of tumor cells that leads to recurrence (40). Herszfeld et al. linked CD30 expression to enhanced tumorigenic features among transformed hematopoietic stem cells (10). Because CD30 expression is retained by

putative EC stem cells identified as SP cells (24), targeting this molecule with CAR T cells may prove advantageous for overcoming the drug resistance of these tumor cells.

The observed Fas-FasL interaction between ECs and CD30.CAR T cells may represent a way to overcome tumor escape associated with antigen heterogeneity. We observed that CD30.CAR T cells can target $CD30^-$ EC cells in a contact-dependent manner via Fas/FasL interaction. While eradicating $CD30^+$ EC cells via perforin/granzyme B-mediated mechanisms, CD30.CAR T cells also upregulate FasL and eliminate surrounding $CD30^-$ tumor cells, if they express the CD95 molecule, via caspase 3 activation. The Fas/FasL pathway is relevant in tumor immunology (41), and Fas agonist mAbs have been developed to activate the apoptotic cascade in tumor cells (42). However, this strategy was not clinically developed due to the systemic toxicities caused by the nonselective targeting of CD95-expressing cells in normal tissues, such as hepatocytes (43). In this regard, the FasL mechanism exploited by CAR T cells, which is cell-cell contact dependent, is more regulated than systemic Fas targeting by mAbs, since upregulation of FasL by CAR T cells only occurs at the tumor site after antigen-specific engagement.

Although our data indicate that the Fas/FasL pathway is critical for CD30.CAR T cells to eliminate surrounding $antigen^{neg}$ tumor cells, tumor cells can still escape immune cell targeting due to tumor-associated dysfunctions of the Fas/Fas-L pathway. For example, tumor cells can downregulate Fas by competition of Fas isoforms or impairment of surface Fas expression (41) or, in the case of EC, develop non-functional Fas mutations (44). In the examples of tumor escape due to alternatively spliced isoforms (5) or antigen loss (6) after CAR T-cell therapy, it is also plausible that endogenous Fas is dysfunctional in these tumors and thus CAR T cells are unable to eliminate $antigen^{neg}$ tumor cells using the Fas/Fa-L mechanism. The EC cell line NCCIT and the neuroblastoma cell line SH-SY5Y are examples of Fas^- tumor cell lines. We observed that these cell lines are indeed more resistant to the cytolytic activity of CD30.CAR T cells. This effect can be reversed, however, by promoting the expression of functional Fas in tumor cells. These data thus highlight a strategy to exploit the Fas/FasL pathway in adoptive T-cell immunotherapy and specifically in CAR T-cell therapies. For example, a clinical translation of the effect we have described may be achieved by the use of oncolytic viruses engineered to promote the expression of functional CD95 in tumor cells *in vivo*, which would further extend our previous observation that armed oncolytic viruses and CAR T cells can cooperate in attacking the tumor (45).

Although effective in targeting $CD30^+$, $CD30^-$ EC cells, and EC stem-like EC cells *in vitro*, CD30.CAR T cells did not completely eradicate EC tumors *in vivo* in our aggressive EC model in which the tumor is engrafted within the kidney. CD30.CAR T cells upon i.v. inoculation localized at the tumor and showed some expansion within the tumor. However, the observed localization, expansion and persistence of CD30.CAR T cells in our model was unable to fully eradicate the tumor. Several strategies have been proposed to further enhance CAR T-cell migration, infiltration and persistence within the tumor, such as engineering CAR T cells to express heparanase to degrade tumor extracellular matrix (21) or constitutive expression of cytokines (46). In addition, combination with other agents may also improve the antitumor activity of CAR T cells. For instance, PD-L1 is expressed in some EC tumors (47). Although PD1/PD-L1 blockades may not be effective as single agents in TGCTs due to

its low mutation rates (48), these inhibitors may prevent the exhaustion of CD30.CAR T cells that express PD1 upon activation (49).

In summary, our data suggest that CD30.CAR T cells represent a clinically applicable immunotherapy strategy for patients with ECs. We demonstrated that CD30.CAR T cells are effective against ECs targeting both differentiated and stem cell-like EC cells. We also highlighted the relevance of the Fas/FasL pathway in CAR T-cell function and how this pathway can be exploited to counter tumor escape due to the downregulation of the targeted antigen by tumor cells, as well as to enhance cytolytic activity of CAR T cells. Finally, because CD30 is expressed in other solid tumors such as neoplasms with chondroid differentiation, which have dismal outcomes (50), CD30.CAR T cells represent a promising treatment avenue for other $CD30^+$ non-lymphomatous malignancies.

Supplementary Material

Refer to Web version on PubMed Central for supplementary material.

Acknowledgments

Lee K. Hong is a recipient of the Gertrude B. Elion Mentored Medical Student Research Award of Triangle Community Foundation. The imaging core and UNC Flow Cytometry core facilities are supported in part by an NCI cancer core grant, P30-CA016086-40. This work was supported by UNC UCRF funds. Dr. Savoldo is supported by a NHLBI grant (R01HL114564) and a Hyundai Hope on Wheel foundation grant.

References

(1). Fesnak AD, June CH, Levine BL. Engineered T cells: the promise and challenges of cancer immunotherapy. Nat Rev Cancer 2016; 16(9):566–581. [PubMed: 27550819]

(2). Dotti G, Gottschalk S, Savoldo B, Brenner MK. Design and development of therapies using chimeric antigen receptor-expressing T cells. Immunol Rev 2014; 257(1):107–126. [PubMed: 24329793]

(3). Gilbert DC, Al-Saadi R, Thway K, Chandler I, Berney D, Gabe R et al. Defining a New Prognostic Index for Stage I Nonseminomatous Germ Cell Tumors Using CXCL12 Expression and Proportion of Embryonal Carcinoma. Clin Cancer Res 2016; 22(5):1265–1273. [PubMed: 26453693]

(4). Sadelain M, Brentjens R, Riviere I. The basic principles of chimeric antigen receptor design. Cancer Discov 2013; 3(4):388–398. [PubMed: 23550147]

(5). Sotillo E, Barrett DM, Black KL, Bagashev A, Oldridge D, Wu G et al. Convergence of Acquired Mutations and Alternative Splicing of CD19 Enables Resistance to CART-19 Immunotherapy. Cancer Discov 2015; 5(12):1282–1295. [PubMed: 26516065]

(6). O'Rourke DM, Nasrallah MP, Desai A, Melenhorst JJ, Mansfield K, Morrissette JJD et al. A single dose of peripherally infused EGFRvIII-directed CAR T cells mediates antigen loss and induces adaptive resistance in patients with recurrent glioblastoma. Sci Transl Med 2017; 9(399).

(7). Zah E, Lin MY, Silva-Benedict A, Jensen MC, Chen YY. T Cells Expressing CD19/CD20 Bispecific Chimeric Antigen Receptors Prevent Antigen Escape by Malignant B Cells. Cancer Immunol Res 2016; 4(6):498–508. [PubMed: 27059623]

(8). Oosterhuis JW, Looijenga LH. Testicular germ-cell tumours in a broader perspective. Nat Rev Cancer 2005; 5(3):210–222. [PubMed: 15738984]

(9). Jacobsen GK, Barlebo H, Olsen J, Schultz HP, Starklint H, Sogaard H et al. Testicular Germ Cell l Tumours in Denmark 1976–1980 Pathology of 1058 Consecutive Cases. Acta Radiologica: Oncology 1984; 23(4):239–247. [PubMed: 6093440]

(10). Herszfeld D, Wolvetang E, Langton-Bunker E, Chung TL, Filpczyk AA, Houssami S et al. CD30 is a survival factor and a biomarker for transformed human pluripotent stem cells. Nat Biotechnol 2006; 24(3):351–357. [PubMed: 16501577]

(11). Giannatempo P, Paolini B, Miceli R, Raggi D, Nicolai N, Fare E et al. Persistent CD30 expression by embryonal carcinoma in the treatment time course: prognostic significance of a worthwhile target for personalized treatment. J Urol 2013; 190(5):1919–1924. [PubMed: 23624209]

(12). Wang CM, Wu ZQ, Wang Y, Guo YL, Dai HR, Wang XH et al. Autologous T Cells Expressing CD30 Chimeric Antigen Receptors for Relapsed or Refractory Hodgkin Lymphoma: An Open-Label Phase I Trial. Clin Cancer Res 2017; 23(5):1156–1166. [PubMed: 27582488]

(13). Ramos CA, Ballard B, Zhang H, Dakhova O, Gee AP, Mei Z et al. Clinical and immunological responses after CD30-specific chimeric antigen receptor-redirected lymphocytes. J Clin Invest 2017; 127(9):3462–3471. [PubMed: 28805662]

(14). Dotti G, Savoldo B, Pule M, Straathof KC, Biagi E, Yvon E et al. Human cytotoxic T lymphocytes with reduced sensitivity to Fas-induced apoptosis. Blood 2005; 105(12):4677–4684. [PubMed: 15713795]

(15). Di Stasi A, De AB, Rooney CM, Zhang L, Mahendravada A, Foster AE et al. T lymphocytes coexpressing CCR4 and a chimeric antigen receptor targeting CD30 have improved homing and antitumor activity in a Hodgkin tumor model. Blood 2009; 113(25):6392–6402. [PubMed: 19377047]

(16). Savoldo B, Rooney CM, Di SA, Abken H, Hombach A, Foster AE et al. Epstein Barr virus specific cytotoxic T lymphocytes expressing the anti-CD30zeta artificial chimeric T-cell receptor for immunotherapy of Hodgkin disease. Blood 2007; 110(7):2620–2630. [PubMed: 17507664]

(17). Savoldo B, Ramos CA, Liu E, Mims MP, Keating MJ, Carrum G et al. CD28 costimulation improves expansion and persistence of chimeric antigen receptor-modified T cells in lymphoma patients. J Clin Invest 2011; 121(5):1822–1826. [PubMed: 21540550]

(18). Xu Y, Zhang M, Ramos CA, Durett A, Liu E, Dakhova O et al. Closely related T-memory stem cells correlate with in vivo expansion of CAR.CD19-T cells and are preserved by IL-7 and IL-15. Blood 2014; 123(24):3750–3759. [PubMed: 24782509]

(19). Pule MA, Straathof KC, Dotti G, Heslop HE, Rooney CM, Brenner MK. A chimeric T cell antigen receptor that augments cytokine release and supports clonal expansion of primary human T cells. Mol Ther 2005; 12(5):933–941. [PubMed: 15979412]

(20). Douglas ML, Boucaut KJ, Antalis TM, Higgins C, Pera MF, Stuttgen MA et al. An orthotopic xenograft model of human nonseminomatous germ cell tumour. British Journal of Cancer 2001; 85:608–611. [PubMed: 11506503]

(21). Caruana I, Savoldo B, Hoyos V, Weber G, Liu H, Kim ES et al. Heparanase promotes tumor infiltration and antitumor activity of CAR-redirected T lymphocytes. Nat Med 2015; 21(5):524–529. [PubMed: 25849134]

(22). Drexler HG, Leber BF, Norton J, Yaxley J, Tatsumi E, Hoffbrand AV et al. Genotypes and immunophenotypes of Hodgkin's disease-derived cell lines. Leukemia 1988; 2(6):371–376. [PubMed: 3131596]

(23). Wang T, Shigdar S, Gantier MP, Hou Y, Wang L, Li Y et al. Cancer stem cell targeted therapy: progress amid controversies. Oncotarget 2015; 6(42):44191–44206. [PubMed: 26496035]

(24). Hirschmann-Jax C, Foster AE, Wulf GG, Nuchtern JG, Jax TW, Gobel U et al. A distinct "side population" of cells with high drug efflux capacity in human tumor cells. Proc Natl Acad Sci U S A 2004; 101(39):14228–14233. [PubMed: 15381773]

(25). Ding XW, Wu JH, Jiang CP. ABCG2: a potential marker of stem cells and novel target in stem cell and cancer therapy. Life Sci 2010; 86(17–18):631–637. [PubMed: 20159023]

(26). Clark AT. The stem cell identity of testicular cancer. Stem Cell Rev 2007; 3(1):49–59. [PubMed: 17873381]

(27). Bosl GJ, Motzer RJ. Testicular germ-cell cancer. N Engl J Med 1997; 337(4):242–253. [PubMed: 9227931]

(28). Waring P, Mullbacher A. Cell death induced by the Fas/Fas ligand pathway and its role in pathology. Immunol Cell Biol 1999; 77(4):312–317. [PubMed: 10457197]

(29). Kunkele A, Johnson AJ, Rolczynski LS, Chang CA, Hoglund V, Kelly-Spratt KS et al. Functional Tuning of CARs Reveals Signaling Threshold above Which CD8+ CTL Antitumor Potency Is Attenuated due to Cell Fas-FasL-Dependent AICD. Cancer Immunol Res 2015; 3(4):368–379. [PubMed: 25576337]

(30). Haynes NM, Smyth MJ, Kershaw MH, Trapani JA, Darcy PK. Fas-ligand-mediated lysis of erbB-2-expressing tumour cells by redirected cytotoxic T lymphocytes. Cancer Immunol Immunother 1999; 47(5):278–286. [PubMed: 10022472]

(31). Saini RV, Wilson C, Finn MW, Wang T, Krensky AM, Clayberger C. Granulysin delivered by cytotoxic cells damages endoplasmic reticulum and activates caspase-7 in target cells. J Immunol 2011; 186(6):3497–3504. [PubMed: 21296981]

(32). Andrade F, Roy S, Nicholson D, Thornberry N, Rosen A, Casciola-Rosen L. Granzyme B directly and efficiently cleaves several downstream caspase substrates: implications for CTL-induced apoptosis. Immunity 1998; 8(4):451–460. [PubMed: 9586635]

(33). Mirzaei HR, Rodriguez A, Shepphird J, Brown CE, Badie B. Chimeric Antigen Receptors T Cell Therapy in Solid Tumor: Challenges and Clinical Applications. Front Immunol 2017; 8:1850. [PubMed: 29312333]

(34). Newick K, Moon E, Albelda SM. Chimeric antigen receptor T-cell therapy for solid tumors. Mol Ther Oncolytics 2016; 3:16006. [PubMed: 27162934]

(35). Chovanec M, Hanna N, Cary KC, Einhorn L, Albany C. Management of stage I testicular germ cell tumours. Nat Rev Urol 2016; 13(11):663–673. [PubMed: 27618772]

(36). Abouassaly R, Fossa SD, Giwercman A, Kollmannsberger C, Motzer RJ, Schmoll HJ et al. Sequelae of treatment in long-term survivors of testis cancer. Eur Urol 2011; 60(3):516–526. [PubMed: 21684072]

(37). Carver BS, Motzer RJ, Kondagunta GV, Sogani PG, Sheinfeld J. Late relapse of testicular germ cell tumors. Urol Oncol 2005; 23(6):441–445. [PubMed: 16301125]

(38). Albany C, Feldman DR, Garbo LE, Einhorn LH. Antitumor activity of brentuximab vedotin in CD30 positive refractory germ cell tumors. J Clin Oncol 2013; 31[suppl. 6]:327.

(39). Necchi A, Anichini A, Raggi D, Giannatempo P, Magazzu D, Nicolai N et al. Brentuximab Vedotin in CD30-Expressing Germ Cell Tumors After Chemotherapy Failure. Clin Genitourin Cancer 2016; 14(4):261–264. [PubMed: 27105722]

(40). Werbowetski-Ogilvie TE, Bhatia M. Pluripotent human stem cell lines: what we can learn about cancer initiation. Trends Mol Med 2008; 14(8):323–332. [PubMed: 18635398]

(41). O' Reilly E, Tirincsi A, Logue SE, Szegezdi E. The Janus Face of Death Receptor Signaling during Tumor Immunoediting. Front Immunol 2016; 7:446. [PubMed: 27843441]

(42). Trauth BC, Klas C, Peters AM, Matzku S, Moller P, Falk W et al. Monoclonal antibody-mediated tumor regression by induction of apoptosis. Science 1989; 245(4915):301–305. [PubMed: 2787530]

(43). Galle PR, Hofmann WJ, Walczak H, Schaller H, Otto G, Stremmel W et al. Involvement of the CD95 (APO-1/Fas) receptor and ligand in liver damage. J Exp Med 1995; 182(5):1223–1230. [PubMed: 7595193]

(44). Takayama H, Takakuwa T, Tsujimoto Y, Tani Y, Nonomura N, Okuyama A et al. Frequent Fas gene mutations in testicular germ cell tumors. Am J Pathol 2002; 161(2):635–641. [PubMed: 12163388]

(45). Nishio N, Diaconu I, Liu H, Cerullo V, Caruana I, Hoyos V et al. Armed oncolytic virus enhances immune functions of chimeric antigen receptor-modified T cells in solid tumors. Cancer Res 2014; 74(18):5195–5205. [PubMed: 25060519]

(46). Hoyos V, Savoldo B, Quintarelli C, Mahendravada A, Zhang M, Vera J et al. Engineering CD19-specific T lymphocytes with interleukin-15 and a suicide gene to enhance their anti-lymphoma/leukemia effects and safety. Leukemia 2010; 24(6):1160–1170. [PubMed: 20428207]

(47). Fankhauser CD, Curioni-Fontecedro A, Allmann V, Beyer J, Tischler V, Sulser T et al. Frequent PD-L1 expression in testicular germ cell tumors. Br J Cancer 2015; 113(3):411–413. [PubMed: 26171934]

(48). Litchfield K, Levy M, Huddart RA, Shipley J, Turnbull C. The genomic landscape of testicular germ cell tumours: from susceptibility to treatment. Nat Rev Urol 2016; 13(7):409–419. [PubMed: 27296647]

(49). Gargett T, Yu W, Dotti G, Yvon ES, Christo SN, Hayball JD et al. GD2-specific CAR T Cells Undergo Potent Activation and Deletion Following Antigen Encounter but can be Protected From Activation-induced Cell Death by PD-1 Blockade. Mol Ther 2016; 24(6):1135–1149. [PubMed: 27019998]

(50). Cheng J, Zhu H, Choi JK. CD30 Expression in Pediatric Neoplasms, Study of 585 Cases. Pediatr Dev Pathol 2017; 20(3):191–196. [PubMed: 28521633]

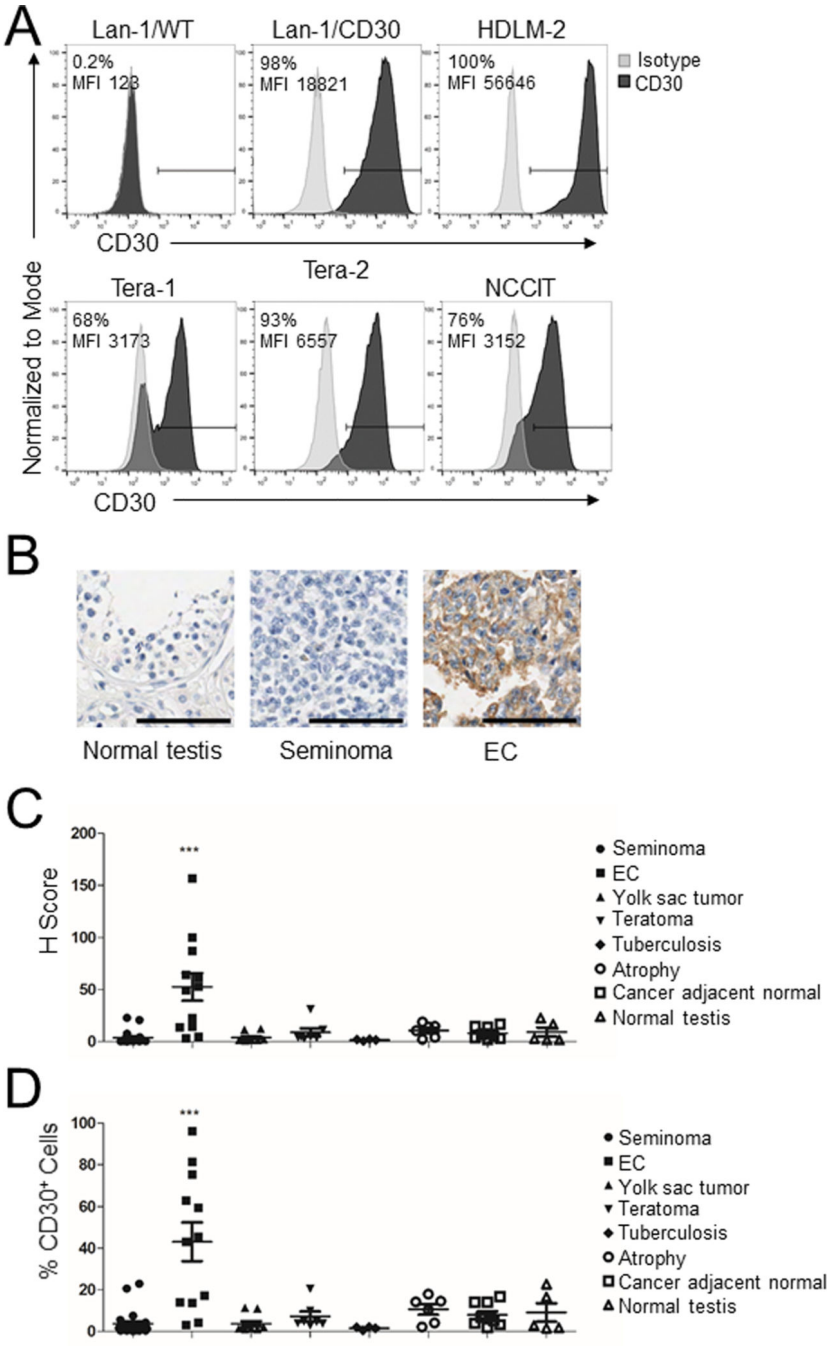

Figure 1. CD30 is expressed by EC cell lines and primary ECs.

(A) CD30 expression was detected on EC tumor cell lines Tera-1, Tera-2 and NCCIT by flow cytometry using anti-human CD30 (Clone Ber-H3). The neuroblastoma cell lines Lan-1/WT and Lan-1/CD30 were used as CD30 negative and positive control, respectively. The Hodgkin's lymphoma cell line HDLM-2 was used as a naturally-expressing CD30 control tumor cell line. Frequency of positive cells and mean fluorescent intensity (MFI) are indicated. (B) Representative IHC for CD30 expression with nuclear counterstain in human tissue microarray (TMA) including normal testes, seminoma (stage I T1N0M0), and ECs

(stage I T2N0M0) at 10X magnification, scale bar=100μm. IHC was performed using anti-human CD30 (Clone Ber-H2). (C,D) Cumulative analysis of CD30 expression for the TMA shown as H score (C), an algorithm calculated based on membrane staining frequency and intensity, or as frequency of positive cells (D). For both panels, each data point represents one tissue sample with mean ± SEM for each group of tissues/tumors. ***=$p<0.001$, one-way ANOVA.

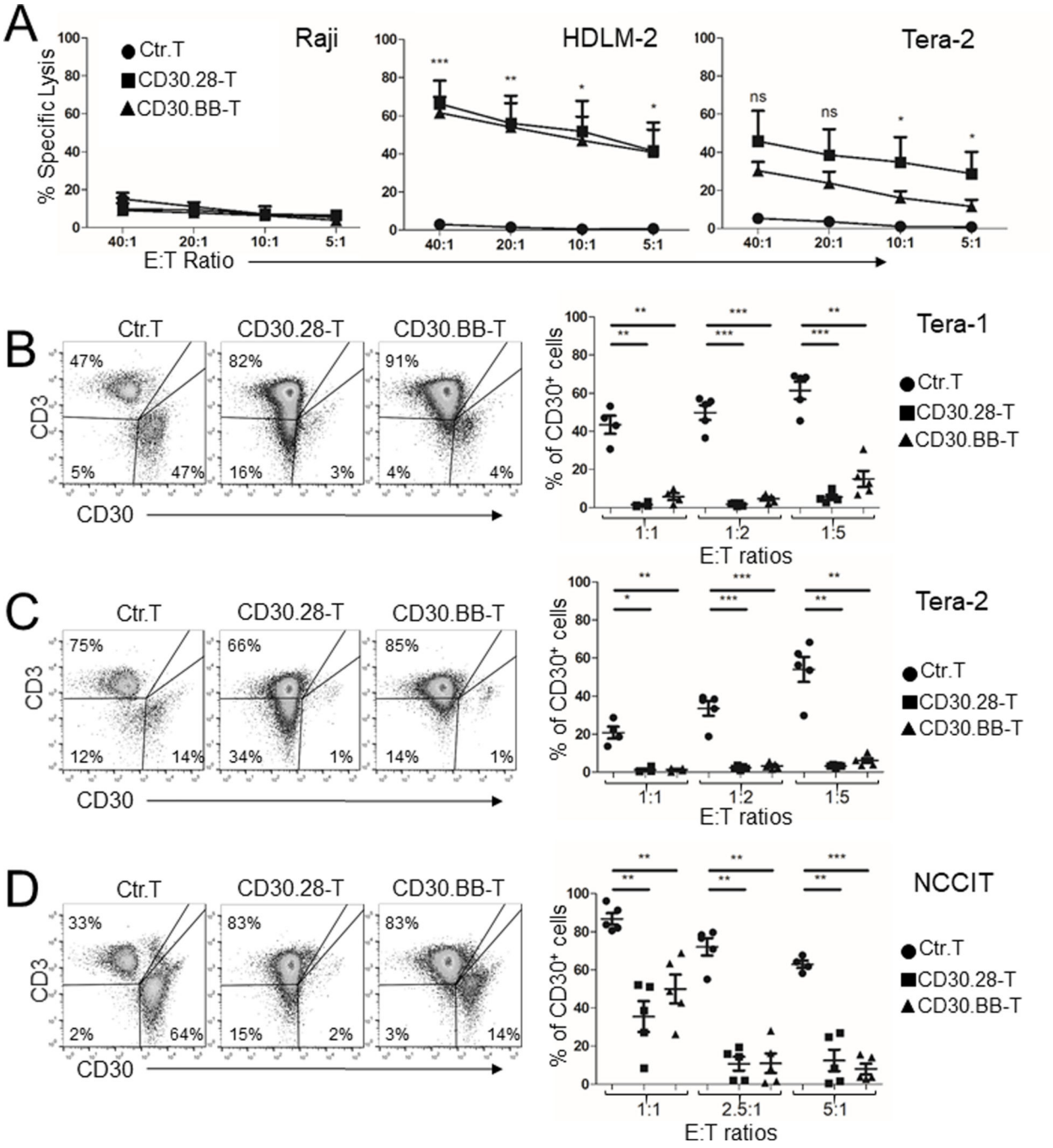

Figure 2. CD30.CAR T cells exhibit cytotoxic activity against EC cell lines *in vitro*.

(A) ^{51}Cr release assay of control T cells (Ctr.T), CD30.28 T cells and CD30.BB T cells against tumor cell lines indicated (mean ± SEM, n = 4 independent experiments). ns=not significant, *=p<0.05, **=p<0.01, ***=p<0.001, repeated measures one-way ANOVA comparing individual effector:target (E:T) ratios. (B-D) Control T cells or CD30.CAR T cells were cocultured with the EC cell line Tera-1 (B), Tera-2 (C) or NCCIT (D). By day 5, remaining EC cells (CD30$^+$) and T cells (CD3$^+$) were collected and analyzed by flow cytometry. Representative flow plots at 1:1 (B,C) or 5:1 (D) E:T ratios (left panels) and

cumulative data for remaining frequency of $CD30^+$ cells for all E:T ratios tested (right panels) are shown (mean ± SEM, n = 4–5 independent experiments). *=p<0.05, **=p<0.01, ***=p<0.001, two-sided, paired Student's T test.

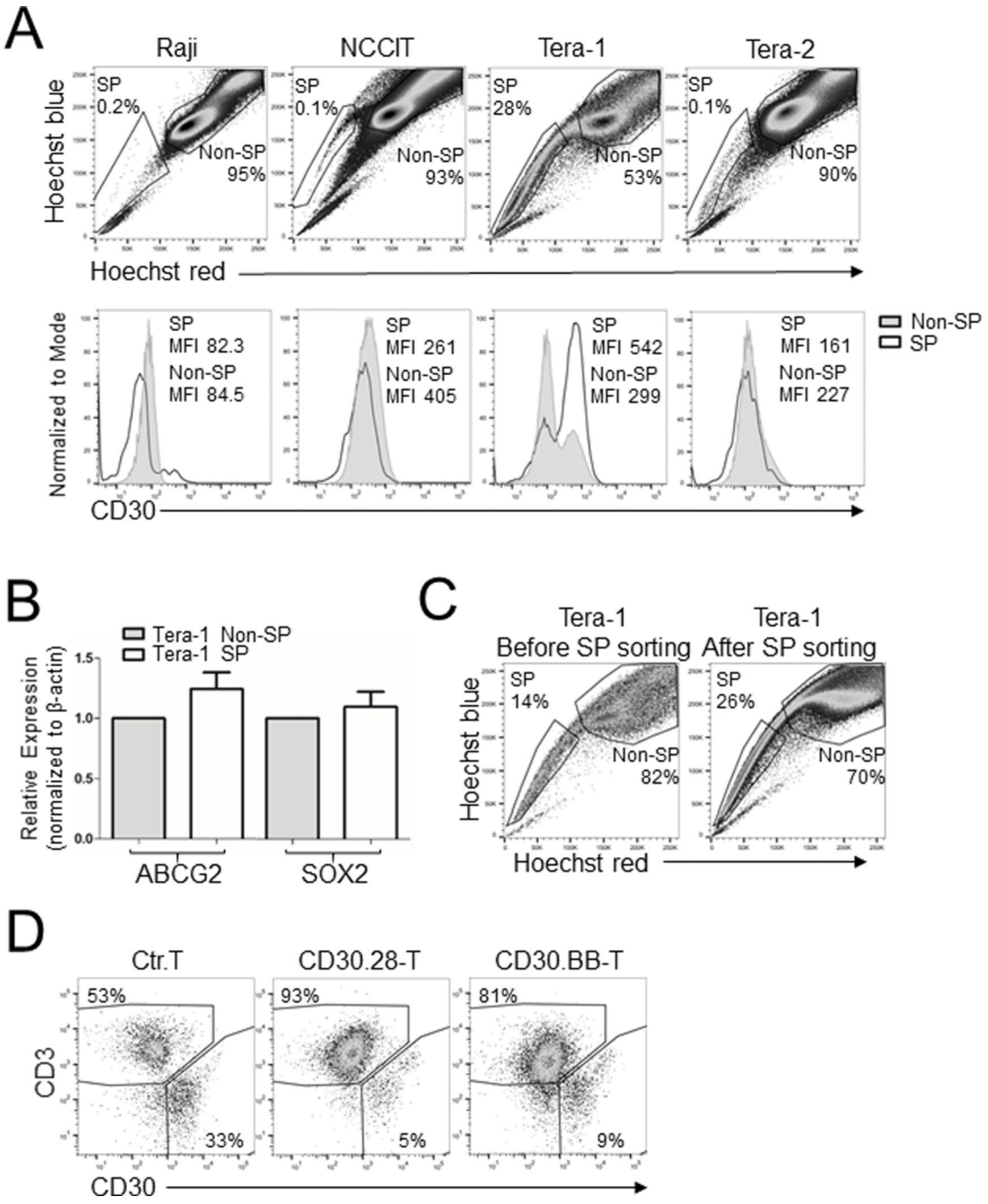

Figure 3. EC-derived SP cells are targeted by CD30.CAR T cells.

(A) Flow cytometry plots of Hoechst 33342-stained tumor cell lines in which percentages of SP and non-SP cells are shown for each tumor cell line (upper panels). Histograms of CD30 expression and MFI on pre-gated SP and non-SP cells are shown (lower panels). Raji cells were used as $CD30^{-}$ control cells. (B) Tera-1 SP and non-SP cells were identified by dye cycle violet staining and FACS-sorted. RNA was extracted, retro-transcribed and amplified by RT-qPCR to measure the expression of the stem cell markers ABCG2 and SOX2. Each bar represents the mean ± SEM of three biological replicates. (C) SP cells were sorted from

the Tera-1 cell line and cultured *in vitro* for 6 weeks. SP-sorted cells regenerated both SP and non-SP cells. (D) Control T cells or CD30.CAR T cells were cocultured with SP-sorted Tera-1 cells at a 1:1 E:T ratio for 5 days, followed by flow cytometry analysis to detect remaining $CD3^+$ T cells and $CD30^+$ tumor cells. Flow cytometry plots of one representative independent experiment are shown (n = 2).

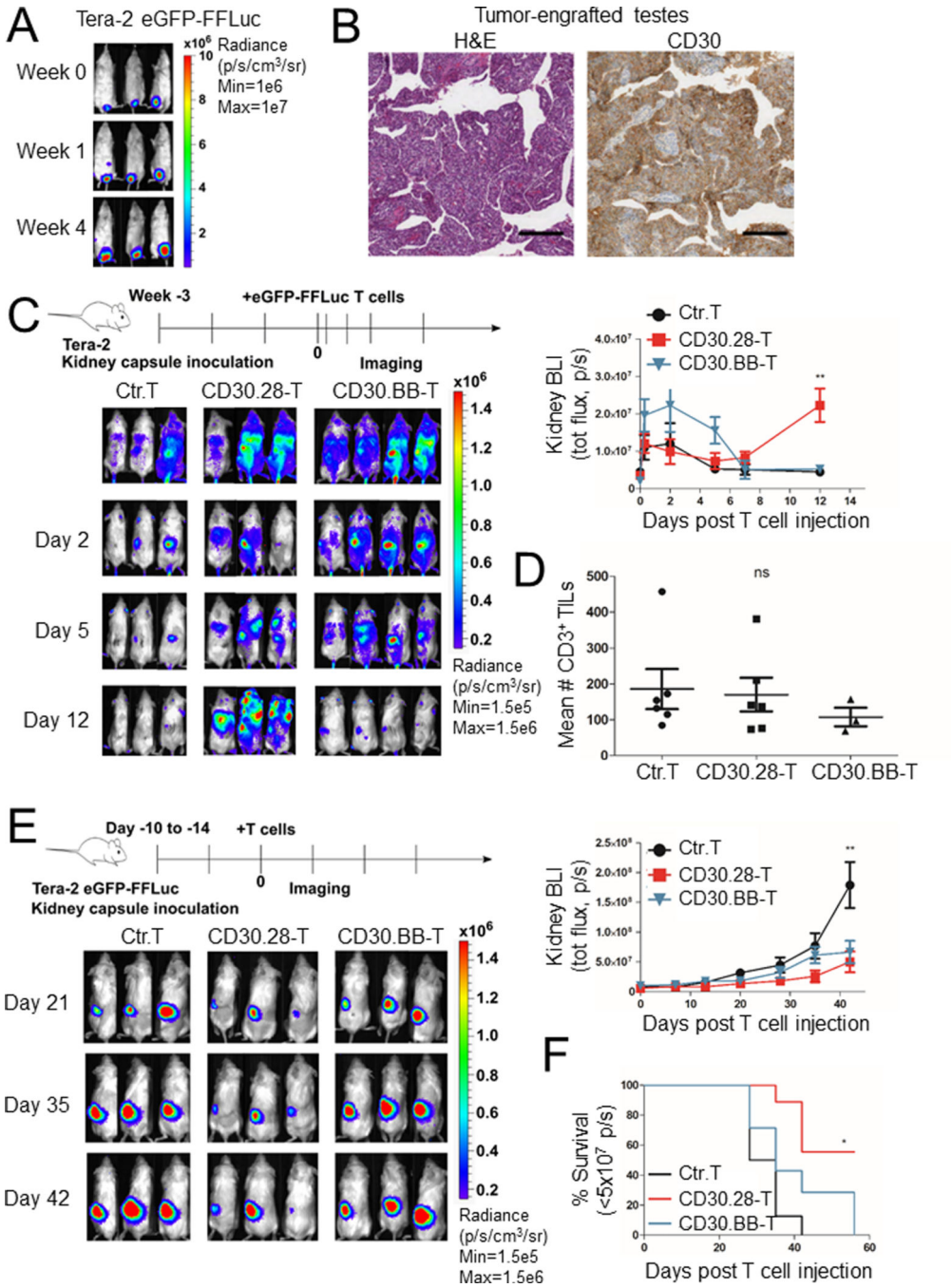

Figure 4. CD30.CAR T cells localize to EC tumors and exhibit antitumor activity *in vivo*.

(A) Representative *in vivo* IVIS imaging of NSG mice inoculated with 2×10^6 Tera-2 cells labeled with eGFP-FFLuc into the left testis. (B) Representative hematoxylin/eosin (H&E) and human CD30 IHC staining of EC tumors growing in the testis are shown at 4X magnification, scale bar=250 μm. (C) NSG mice were inoculated with Tera-2 cells under the left kidney capsule and, 21 days later, infused i.v. with 1×10^7 eGFP-FFLuc-labeled CD30.CAR T cells or CD19.CAR T cells (irrelevant T cells). Representative IVIS images indicating CAR T-cell localization and expansion (left panel) and cumulative BLI (right

panel) are shown (mean ± SEM, n=3–4 per group, 2 independent experiments). **=p<0.001, one-way ANOVA at day 12. (D) T-cell treated mice were sacrificed at day 30–45 post tumor inoculation and tumors were stained with anti-human CD3 to detect tumor-infiltrating T lymphocytes. $CD3^+$ T cells were counted at 400x magnification with the tumor covering at least 80% of the field of view in a blinded fashion. Cumulative quantification of $CD3^+$ T-cell counts are shown (mean ± SEM, n=1–3 per group, 4 independent experiments). ns=not significant, one-way ANOVA. (E) NSG mice were inoculated with Tera-2 cells labeled with eGFP-FFLuc under the left kidney capsule and received 1×10^7 CD30.CAR T cells or CD19.CAR T cells (Ctr.T) i.v. by day 15. Representative IVIS images indicating tumor growth (left panel) and cumulative BLI (right panel) are illustrated (mean ± SEM, n = 4–5 per group, 2 independent experiments). **=p<0.001, one-way ANOVA at day 42. (F) Cumulative Kaplan-Meier survival curve of BLI $<5 \times 10^7$ p/s for 2 independent experiments. *=p<0.05 by log-rank (Mantel-Cox) test.

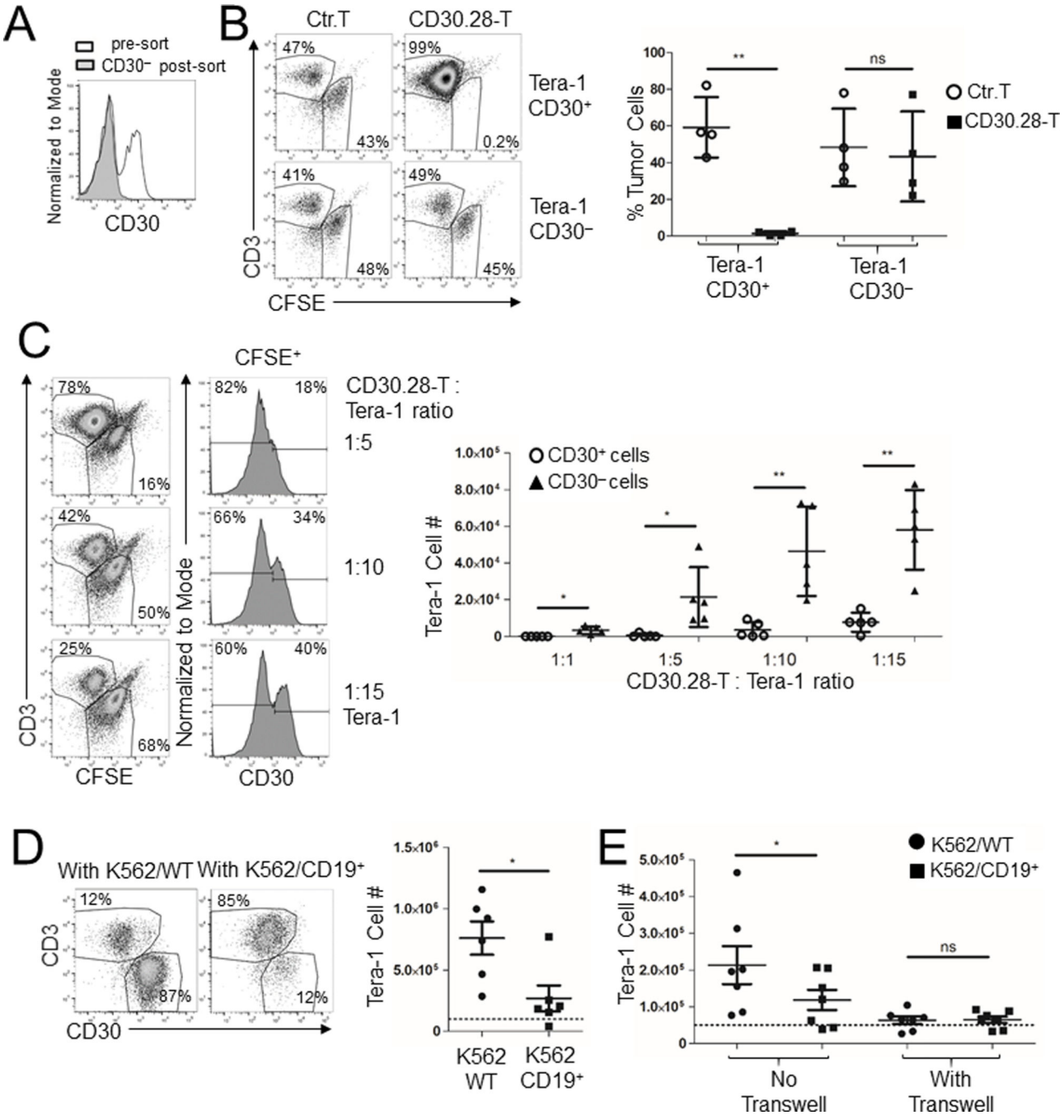

Figure 5. CD30.CAR T cells eliminate Tera-1 CD30⁻ cells in a cell contact-dependent but antigen-independent manner.

(A) Tera-1 cells were FACS-sorted to obtain $CD30^+$ and $CD30^-$ cells. Histogram shows CD30 expression on sorted cells. (B) Sorted Tera-1 $CD30^+$ and $CD30^-$ cells were labeled with CFSE and cocultured with either control T cells or CD30.28 T cells for 5 days. Cells were then collected and evaluated by flow cytometry to quantify T cells ($CD3^+$) and tumor cells ($CFSE^+$). Representative flow plots (top panels) and cumulative data (bottom panels) summarizing $CFSE^+$ tumor cell frequency (mean ± SEM, n = 4 independent experiments) are shown. ns = not significant, **=p<0.01, two-sided, paired Student's T test. (C) Tera-1

cells were labeled with CFSE and cocultured for 5 days with CD30.28 T cells at decreasing E:T ratios ranging from 1:1 to 1:15. Representative plots (left columns) and CD30 histograms (right columns) of $CFSE^+$ Tera-1 cells with cumulative data (right graph) for remaining tumor cells calculated with flow cytometry-based counting beads are shown (mean ± SEM, n = 5 independent experiments). *=p<0.05, **=p<0.01, two-sided, paired Student's T test. (D) Tera-1 cells were cocultured with CD19.CAR T cells in the presence of either K562/WT or K562/$CD19^+$ cells at 1:1:1 ratio for 5 days. Cells were then collected and evaluated by flow cytometry to quantify T cells ($CD3^+$) and tumor cells ($CD30^+$). Shown are representative flow cytometry plots of $CD3^+$ T cells and $CD30^+$ EC cells pre-gated to exclude $CD33^+$ K562 cells (left panels) and cumulative data summarizing tumor cell numbers (right panels). Dashed line represents the initial Tera-1 cell number (mean ± SEM, n=5 independent experiments). *=p<0.05, two-sided, paired Student's T test. (E) Tera-1 cells were plated in the lower chamber of a 0.4μm transwell-plate 24 hours prior to plating CD19.CAR T cells and either K562/WT or K562/$CD19^+$ cells in the upper chamber at 1:1:1 ratio for 5 days. Tera-1 cells in the lower chamber were then collected and counted by flow cytometry. Cumulative data are shown, dashed line represents the initial cell number (mean ± SEM, n = 7 independent experiments). ns = not significant, *=p<0.05, two-sided, paired Student *t* test.

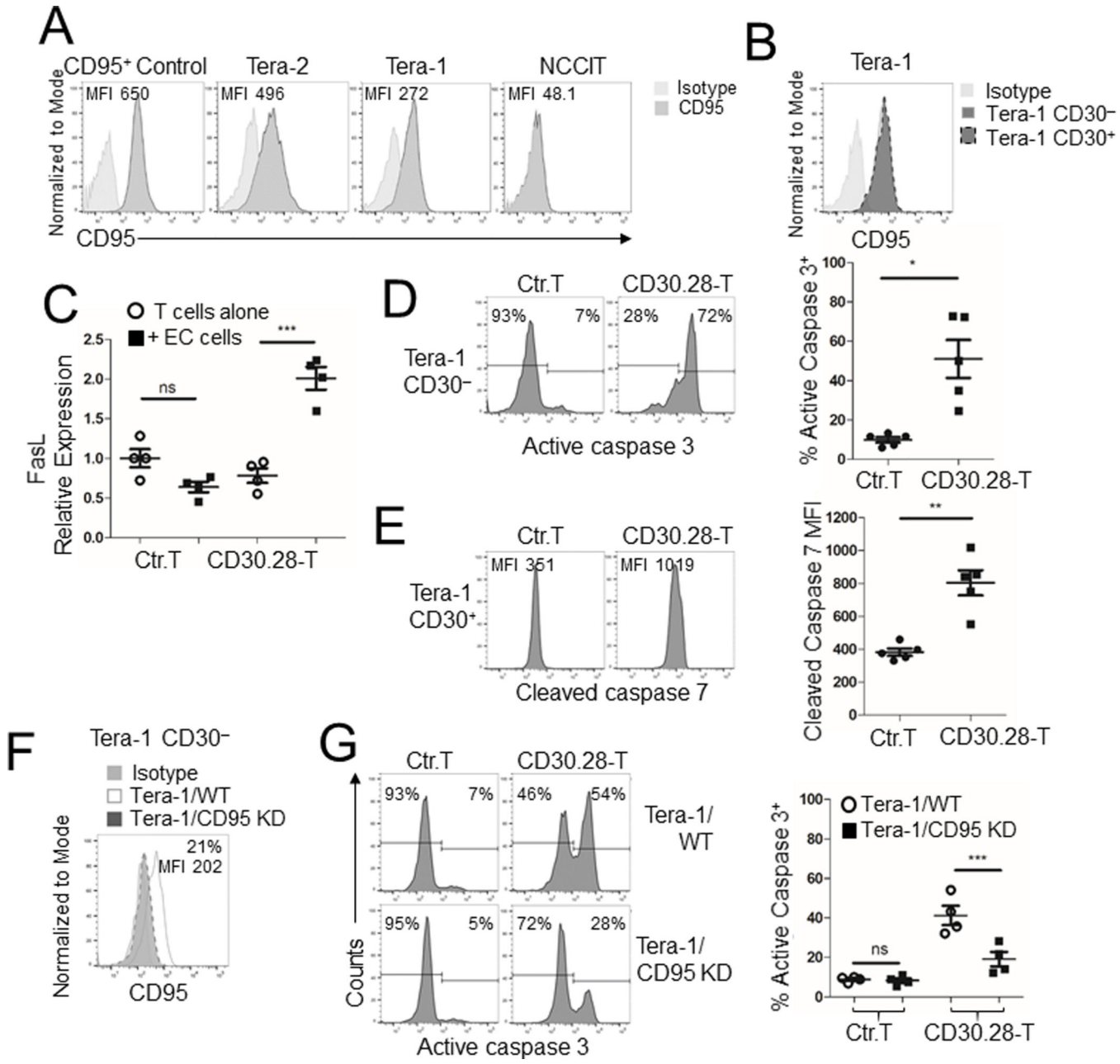

Figure 6. Functional Fas-FasL interaction is critical for the elimination of CD30⁻ EC cells.

(A) Flow cytometry histograms showing CD95 expression and MFI in EC cell lines. T cells stimulated with anti-CD3/CD28 mAbs were used as positive control for CD95 expression. (B) CD95 expression on pre-gated $CD30^+$ or $CD30^-$ Tera-1 cells. (C) RT-qPCR cumulative data for FasL mRNA expression among control T cells or CD30.28 T cells cultured alone or with EC cells at a 5:1 E:T ratio for 4 hours at 37°C (mean ± SEM, n = 6 independent experiments). FasL mRNA expression was normalized to β-actin mRNA. ns = not significant, ***=p<0.0001, two-sided paired Student's T test. (D-E) Active caspase 3 and cleaved caspase 7 were assessed by flow cytometry in Tera-1 cells cocultured with control T cells or CD30.28 T cells at 1:2 or 1:5 E:T ratio for 18 hours, respectively. Representative

flow plots (left panels) and cumulative data (right panels) of active caspase 3 frequency (D) or cleaved caspase 7 MFI (E) among Tera-1 $CD30^-$ and $CD30^+$ cells, respectively are shown (mean ± SEM, n = 5 independent experiments). *=p<0.05, **=p<0.01, two-sided, paired Student's T test. (F) CD95 expression on pre-gated $CD30^-$ cells for Tera-1/WT or Tera-1 cells transduced with CD95 shRNA and FACS-sorted based on $CD95^-$ expression (Tera-1/CD95 KD) is shown. CD95 frequency and MFI for Tera-1/CD95 KD cells are indicated. (G) Tera-1/WT or Tera-1/CD95 KD cells were cocultured with control T cells or CD30.28 T cells at 1:5 E:T ratio for 18 hours. Representative flow plots (left panels) and cumulative data (right panels) for active caspase 3 among Tera-1 $CD30^-$ cells are shown (mean ± SEM, n = 4 independent experiments). ns = not significant, ***=p<0.001, two-sided, paired Student *t* test.

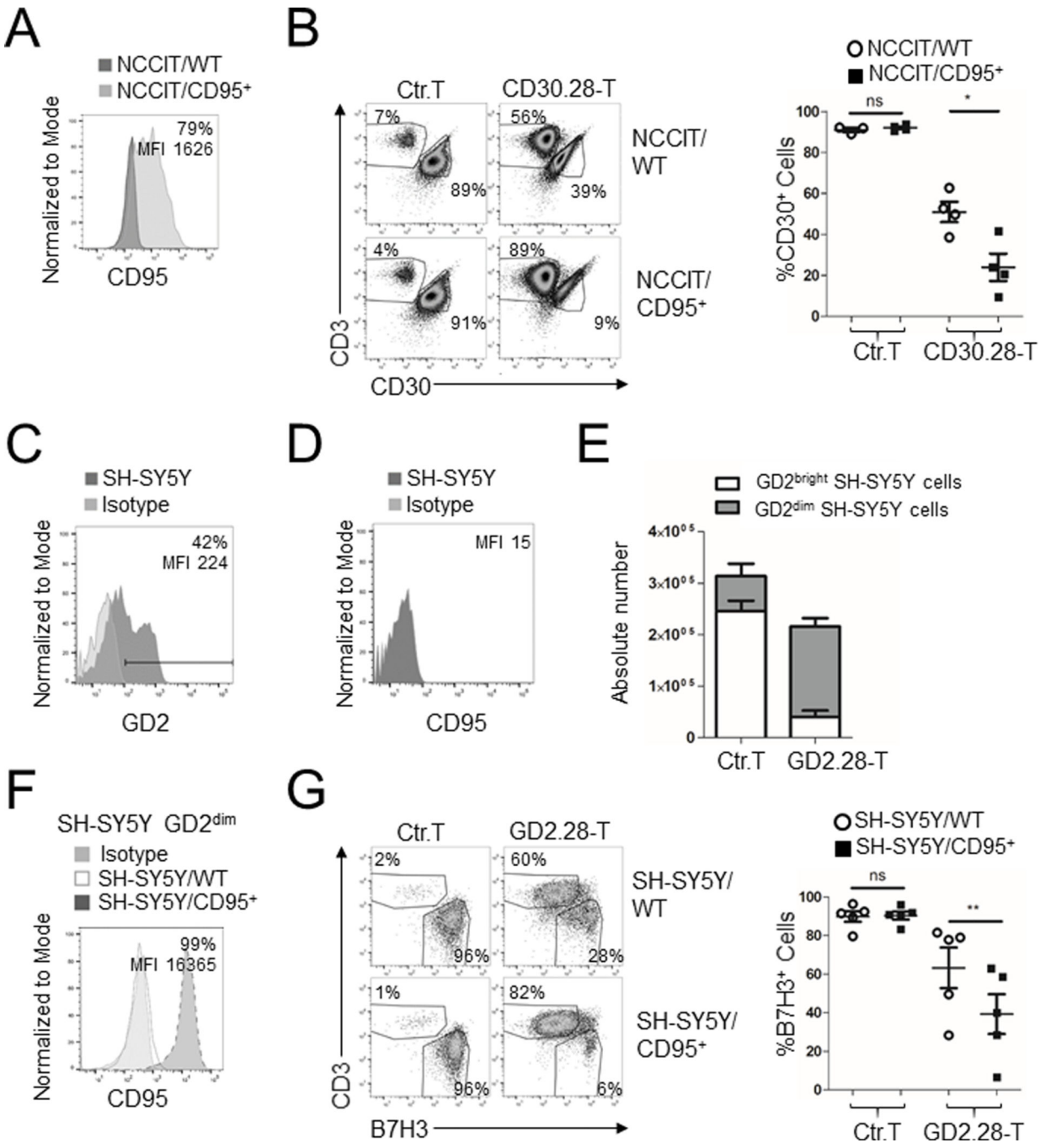

Figure 7. Functional Fas expression is sufficient to improve CAR T-cell activity.

(A) CD95 expression on NCCIT/WT cells and NCCIT cells transduced to express CD95 (NCCIT/CD95$^+$). CD95 frequency and MFI for NCCIT/CD95$^+$cells are indicated. (B) NCCIT/WT or NCCIT/CD95$^+$ cells were cocultured with control T cells or CD30.28 T cells at 1:2 E:T ratio for 5 days. Representative flow plots (left panels) and cumulative data (right panels) showing remaining tumor cells are illustrated (mean ± SEM, n = 4 independent experiments). ns = not significant, *=p<0.05, two-sided, paired Student's T test. (C-D) Flow cytometry histograms showing GD2 (C) or CD95 (D) expression and/or MFI in SH-SY5Y

cells. (E) Control T cells or GD2.CAR T cells were cocultured with SH-SY5Y cells at a 1:5 E:T ratio for 5 days. Remaining tumor cells were collected and absolute numbers of $GD2^{bright}$ and $GD2^{dim}$ cells were calculated by flow cytometry-based counting beads (mean ± SEM, n = 7 independent experiments). (F) CD95 expression pre-gated on $GD2^{dim}$ SH-SY5Y/WT cells and SH-SY5Y cells transduced to express CD95 (SH-SY5Y/$CD95^{+}$). CD95 frequency and MFI for SH-SY5Y/$CD95^{+}$ cells are indicated. (G) SH-SY5Y/WT or SH-SY5Y/$CD95^{+}$ cells were cocultured with control T cells or GD2.28 T cells at 1:5 E:T ratio for 5 days. Representative flow plots (left panels) and cumulative data (right panels) showing remaining tumor cells using B7H3 as a tumor cell marker are illustrated (mean ± SEM, n = 5 independent experiments). ns = not significant, **=$p<0.01$, two-sided, paired Student *t* test.